# Band-to-Band Visible-Light Photon Excitation and Photoactivity Induced by Homogeneous Nitrogen Doping in Layered Titanates

Gang Liu,[†,‡] Lianzhou Wang,[†] Chenghua Sun,[†,§] Xiaoxia Yan,[†] Xuewen Wang,[‡] Zhigang Chen,[‡] Sean C. Smith,[§] Hui-Ming Cheng,*[,‡] and Gao Qing Lu*[,†]

*ARC Centre of Excellence for Functional Nanomaterials, School of Engineering, Centre for Computational Molecular Science, Australian Institute of Bioengineering and Nanotechnology, The University of Queensland, Queensland 4072, Australia, and Shenyang National Laboratory for Materials Science, Institute of Metal Research, Chinese Academy of Sciences, 72 Wenhua Road, Shenyang 110016, China*

*Received November 3, 2008*

The distribution of dopants in semiconductors can intrinsically determine the electronic structure and consequently the absorbance, redox potential, and charge-carrier mobility of the semiconductor photocatalysts. In contrast to most reported nitrogen-doped titania photocatalysts with some localized states in the intrinsic band gap and small visible light absorption shoulders induced by inhomogeneous nitrogen doping near the particle surface, we report here the homogeneous substitution of O by N in the whole particles of layered titanates. The resultant materials $Cs_{0.68}Ti_{1.83}O_{4-x}N_x$ exhibited extraordinary band-to-band excitation in the visible-light ranging up to blue light. From photoelectron spectroscopy and first-principles calculations, the upward shift of valence band maximum by N 2p states is concluded as the cause of the band-to-band visible light excitation. The holes generated upon visible light excitation in the newly formed valence bands of $Cs_{0.68}Ti_{1.83}O_{4-x}N_x$ and $H_{0.68}Ti_{1.83}O_{4-x}N_x$ had strong oxidation ability in oxidizing $OH^-$ into active •OH radicals in photocatalysis. These findings are the clear evidence for the substantial role of homogeneous nitrogen doping in obtaining band-to-band visible-light photon excitation in layered titanates. The new physical insights into the electronic structure of homogeneous substitutional N in layered titanates gained here may have important implications for developing other efficient visible light photocatalysts by nonmetal doping.

## 1. Introduction

The search for active visible-light photocatalysts has been intensifying worldwide, mainly because of the great significance of such photocatalysts in clean energy,[1−10] photoelectrochemical process,[11−16] and environmental applications[17−23] under solar irradiation. To overcome the limitation of UV-only photocatalytic activity of the most promising titania-based photocatalysts for environmental applications, anion doping,[24] especially nitrogen doping, has shown a great potential in increasing visible-light photocatalytic activity. Many routes, such as wet-chemical methods,[25] mechanochemical reactions with organic nitrogen-containing com-

* Corresponding author. E-mail: maxlu@uq.edu.au (G.Q.L.); cheng@imr.ac.cn (H.-M.C.). Tel: 61 7 33653735 (G.Q.L.); +86 24 23971611 (H.-M.C.). Fax: +61 7 33656074 (G.Q.L.); +86 24 23903126 (H.-M.C.).

† ARC Centre of Excellence for Functional Nanomaterials, School of Engineering, and Australian Institute of Bioengineering and Nanotechnology, The University of Queensland.

‡ Shenyang National Laboratory for Materials Science, Institute of Metal Research, Chinese Academy of Sciences.

§ Centre for Computational Molecular Science, Australian Institute of Bioengineering and Nanotechnology, The University of Queensland.

(1) (a) Fujishima, A.; Honda, K. *Nature* **1972**, *238*, 37. (b) Zou, Z.; Ye, J.; Sayama, K.; Arakawa, H. *Nature* **2001**, *414*, 625.
(2) Ishikawa, A.; Takata, T.; Kondo, J.; Hara, M.; Kobayashi, H.; Domen, K. *J. Am. Chem. Soc.* **2002**, *124*, 13547.
(3) Tsuji, I.; Kato, H.; Kobayashi, H.; Kudo, A. *J. Am. Chem. Soc.* **2004**, *126*, 13406.
(4) Maeda, K.; Teramura, K.; Lu, D.; Takata, T.; Saito, N.; Inoue, Y.; Domen, K. *Nature* **2006**, *440*, 216.
(5) Liu, M.; You, W.; Lei, Z.; Zhou, G.; Yang, J.; Wu, G.; Ma, G.; Luan, G.; Takata, T.; Hara, M.; Domen, K.; Li, C. *Chem. Comm.* **2004**, 2192.
(6) Tang, J.; Zou, Z.; Ye, J. *Angew. Chem., Int. Ed.* **2004**, *43*, 4463.
(7) Kim, H.; Hwang, D.; Lee, J. *J. Am. Chem. Soc.* **2004**, *126*, 8912.
(8) Tsuji, I.; Kato, H.; Kudo, A. *Angew. Chem., Int. Ed.* **2005**, *44*, 3565.
(9) Kim, H.; Borse, P.; Choi, W.; Lee, J. *Angew. Chem., Int. Ed.* **2005**, *44*, 4585.
(10) Zong, X.; Yan, H.; Wu, G.; Ma, G.; Wen, F.; Wang, L.; Li, C. *J. Am. Chem. Soc.* **2008**, *130*, 7176.
(11) (a) Grätzel, M. *Nature* **2001**, *414*, 338. (b) Cesar, I.; Kay, A.; Martinez, J. A. G.; Grätzel, M. *J. Am. Chem. Soc.* **2006**, *128*, 4582. (c) Kay, A.; Cesar, I.; Grätzel, M. *J. Am. Chem. Soc.* **2006**, *128*, 15714.
(12) (a) Martinson, A. B. F.; Elam, J. W.; Hupp, J. T.; Pellin, M. J. *Nano Lett.* **2007**, *7*, 2183. (b) Hamann, T. W.; Martinson, A. B. E.; Elam, J. W.; Pellin, M. J.; Hupp, J. T. *Adv. Mater.* **2008**, *20*, 1560.
(13) (a) Martinson, A. B. F.; McGarrah, J. E.; Parpia, M. O. K.; Hupp, J. T. *Phys. Chem. Chem. Phys.* **2006**, *8*, 4655. (b) Martinson, A. B. F.; Hamann, T. W.; Pellin, M. J.; Hupp, J. T. *Chem.-A Europ. J.* **2008**, *14*, 4458.
(14) Zhu, K.; Neale, N. R.; Miedaner, A.; Frank, A. J. *Nano Lett.* **2007**, *7*, 69.
(15) Park, J. H.; Kim, S.; Bard, A. J. *Nano Lett.* **2006**, *6*, 24.
(16) Mor, G. K.; Prakasam, H. E.; Varghese, O. K.; Shankar, K.; Grimes, C. A. *Nano Lett.* **2007**, *7*, 2356.
(17) (a) Linsebigler, A. L.; Lu, G. Q.; Yates, J. T. *Chem. Rev.* **1995**, *95*, 735. (b) Hoffman, M. R.; Martin, S. T.; Choi, W.; Bahnemann, D. W. *Chem. Rev.* **1995**, *95*, 69. (c) Thompson, T. L.; Yates, J. T. *Chem. Rev.* **2006**, *106*, 4428.
(18) (a) Zheng, N.; Bu, X.; Vu, H.; Feng, P. *Angew. Chem., Int. Ed.* **2005**, *44*, 5299. (b) Hagiwara, H.; Onoo, N.; Inoue, T.; Matsumoto, H.; Ishihara, T. *Angew. Chem., Int. Ed.* **2006**, *45*, 1420.
(19) Ritterskamp, P.; Kuklya, A.; Wüstkamp, M.-A.; Kerpen, K.; Weidenthaler, C.; Demuth, M. *Angew. Chem., Int. Ed.* **2007**, *46*, 7770.
(20) Gao, F.; Chen, X.; Yin, K.; Dong, S.; Ren, Z.; Yuan, F.; Tao, Y.; Zou, Z.; Liu, J. *Adv. Mater.* **2007**, *19*, 2889.
(21) Zhang, L.; Djerdj, I.; Cao, M.; Antonietti, M.; Niederberger, M. *Adv. Mater.* **2007**, *19*, 2083.
(22) Kim, T.; Hwang, S.; Jhung, S.; Chang, J.; Park, H.; Choi, W.; Choy, J. *Adv. Mater.* **2008**, *20*, 539.
(23) (a) Abe, R.; Takami, H.; Murakami, N.; Ohtani, B. *J. Am. Chem. Soc.* **2008**, *130*, 7780. (b) Zhao, Z. G.; Miyauchi, M. *Angew. Chem., Int. Ed.* **2008**, *47*, 7051.

10.1021/cm802986r CCC: $40.75 
Published on Web 03/10/2009

pounds or gaseous ammonia,[26] physical methods,[27] thermal treatment in ammonia atmosphere,[28] etc., have been developed to realize the nitrogen doping in $TiO_2$. Depending on the synthesis routes, the properties of nitrogen-doped $TiO_2$ obtained vary substantially. The two key properties of nitrogen-doped $TiO_2$ are the nature of nitrogen dopant and the effect of nitrogen dopant on the electronic structure of $TiO_2$, which can intrinsically determine the photon absorption, redox power, and transport of photoinduced carriers. As for the nature of nitrogen dopant, different N species such as $NO_x$,[29] $NH_x$,[30] and substitutional N[24a,31] has been proposed to be responsible for the visible light activity of nitrogen-doped $TiO_2$. Although the exact identification of nitrogen dopant with its binding energy around 400 eV is still a challenging topic, it is generally accepted that the nitrogen species with its binding energy around 396 eV is attributed to the substitutional N for lattice O atoms.[24a]

To explore the important effect of nitrogen dopant on the electronic structure of $TiO_2$, both theoretical investigations[32] and experimental work[33] have been conducted. Two main hypotheses have been proposed, namely that (i) the up-shifted valence band maximum by N 2p states and/or (ii) the localized states from N 2p states as well as concomitant color centers in the band gap are considered as the origin of visible light absorption. In principle, the former results in a band-to-band visible light absorption edge by exciting electrons in the newly formed valence band to the conduction band, whereas the latter is characterized by a small visible light absorption shoulder and retaining of the pristine absorption edge. Examining the reported experimental work on nitrogen-doped $TiO_2$-based photocatalysts, we found that most cases belong to the latter,[34] with one exception where band-to-band visible light absorption edge in $TiO_2$ films using radio frequency (RF) magnetron sputtering deposition was observed.[35] Significant limitations associated with nitrogen-doped $TiO_2$ photocatalysts with localized states in the intrinsic band gap apparently remain, including both limited visible-light absorbance and lowered mobility of carriers in the localized states, which are the two key factors impairing visible-light photocatalytic activity.[24a]

Fundamentally, this issue can be understood in terms of a limitation in the types of structures that have been realized hitherto in nitrogen-doped $TiO_2$ single crystals. These may be broadly characterized as inhomogeneous distribution of N dopant in the whole particles but only within a subsurface region of very limited depth.[32f] To resolve this problem, we have considered layered titanate with a lepidocrocite structure as the potential starting material for preparing a photocatalyst with a homogeneous nitrogen distribution throughout the entire particles. This choice is based on the following rationale: (i) compared with anatase crystals, layered titanate possesses similar sheets of $TiO_6$ octahedra sharing four edges, but with unique interlayer galleries between the sheets; (ii) the layered galleries could be expected to offer an excellent pathway facilitating the nitriding process and enabling essentially homogeneous nitrogen doping; and (iii) If successful, uniformly distributed nitrogen would obviously

(24) (a) Asahi, R.; Morikawa, T.; Ohwaki, T.; Aoki, K.; Taga, Y. *Science* **2001**, *293*, 269. (b) Khan, S. U. M.; Al-Shahry, M.; Ingler, W. B., Jr. *Science* **2002**, *297*, 2243. (c) Umebayashi, T.; Yamaki, T.; Itoh, H.; Asai, K. *Appl. Phys. Lett.* **2002**, *81*, 454. (d) Zhao, W.; Ma, W.; Chen, C.; Zhao, J.; Shuai, Z. *J. Am. Chem. Soc.* **2004**, *126*, 4782. (e) Sakhivel, S.; Kisch, H. *Angew. Chem., Int. Ed.* **2003**, *42*, 4908. (f) Burda, C.; Lou, Y.; Chen, X.; Samia, A. C.; Stout, S.; Gole, J. J. L. *Nano Lett.* **2003**, *3*, 1049. (g) Li, D.; Haneda, H.; Labhsetwar, N. K.; Hishita, S.; Ohashi, N. *Chem. Phys. Lett.* **2005**, *401*, 579. (h) Ho, W.; Yu, J. C.; Lee, S. *ChemComm* **2006**, 1115. (i) Hong, X.; Wang, Z.; Cai, W.; Lu, F.; Zhang, J.; Yang, Y.; Ma, N.; Liu, Y. *Chem. Mater.* **2005**, *17*, 1548.

(25) (a) Burda, C.; Lou, Y. B.; Chen, X. B.; Samia, A. C. S.; Stout, L.; Gole, J. L. *Nano Lett.* **2003**, *3*, 1049. (b) Sano, T.; Negishi, N.; Koike, K.; Takeuchi, K.; Matsuzawa, S. *J. Mater. Chem.* **2004**, *14*, 380. (c) In, S.; Orlov, A.; Garcia, F.; Tikhov, M.; Wright, D. S.; Lambert, R. M. *Chem. Commun.* **2006**, *40*, 4236.

(26) (a) Yin, S.; Yamaki, H.; Komatsu, M.; Zhang, Q. W.; Wang, J. S.; Tang, Q.; Saito, F.; Sato, T. *J. Mater. Chem.* **2003**, *13*, 2996. (b) Liu, G.; Li, F.; Chen, Z. G.; Lu, G. Q.; Cheng, H. M. *J. Solid State Chem.* **2006**, *179*, 331.

(27) For example: (a) Lindgren, T.; Mwabora, J. M.; Avendano, E.; Jansson, J.; hoel, A.; Granqvist, C. G.; Lindquist, S. E. *J. Phys. Chem. B* **2003**, *107*, 5709. (b) Diwald, O.; Thompson, T. L.; Goralski, E. G.; Walck, S., Jr.; Yates, J. T. *J. Phys. Chem. B* **2004**, *108*, 52. (c) Torres, G. R.; Lindgren, T.; Lu, J.; Granqvist, C. G.; Lindquist, S. E. *J. Phys. Chem. B* **2004**, *108*, 5995. (d) Nakano, Y.; Morikawa, T.; Ohwaki, T.; Taga, Y. *Appl. Phys. Lett.* **2005**, *86*, 132104. (e) Batzill, M.; Morales, E. H.; Diebold, U. *Chem. Phys.* **2007**, *339*, 36. (f) Cheung, S. H.; Nachimuthu, P.; Joly, A. G.; Engelhard, M. H.; Bowman, M. K.; Chambers, S. A. *Surf. Sci.* **2007**, *601*, 1754.

(28) Irie, H.; Watanabe, Y.; Hashimoto, K. *J. Phys. Chem. B* **2003**, *107*, 5483.

(29) (a) Sato, S. *Chem. Phys. Lett.* **1986**, *123*, 126. (b) Sakthivel, S.; Janczarek, M.; Kisch, H. *J. Phys. Chem. B* **2004**, *108*, 19384. (c) Sato, S.; Nakamura, R.; Abe, S. *Appl. Catal., B* **2005**, *284*, 131. (d) Sakatani, Y.; Nunoshige, J.; Ando, H.; Okusako, K.; Koike, H.; Takata, T.; Kondo, J. N.; Hara, M.; Domen, K. *Chem. Lett.* **2003**, *32*, 1156. (e) Di Valentin, C.; Pacchioni, G.; Selloni, A.; Livraghi, S.; Giamello, E. *J. Phys. Chem. B* **2005**, *109*, 11414. (f) Livraghi, S.; Votta, A.; Paganini, M. C.; Giamello, E. *Chem. Comm.* **2005**, *4*, 498.

(30) Diwald, O.; Thompson, T. L.; Zubkov, T.; Goralski, E. G.; Walck, S. D.; Yates, J. T. *J. Phys. Chem. B* **2004**, *108*, 6004.

(31) (a) Miyauchi, M.; Ikezawa, A.; Tobimatsu, H.; Irie, H.; Hashimoto, K. *Phys. Chem. Chem. Phys.* **2004**, *6*, 865. (b) Lin, Z.; Orlov, A.; Lambert, R. M.; Payne, M. C. *J. Phys. Chem. B* **2005**, *109*, 20948. (c) Diwald, O.; Thompson, T. L.; Goralski, E. G.; Walck, S. D.; Yates, J. T. *J. Phys. Chem. B* **2004**, *108*, 52.

(32) For example:(a) Di Valentin, C.; Pacchioni, G.; Selloni, A. *Phys. Rev. B* **2004**, *70*, 085116. (b) Di Valentin, C.; Pacchioni, G. F.; Selloni, A.; Livrahi, S.; Giamello, E. *J. Phys. Chem. B* **2005**, *109*, 11414. (c) Wang, H.; Lewis, J. P. *J. Phys.: Condens. Matter.* **2006**, *18*, 421. (d) Yang, K.; Dai, Y.; Huang, B.; Han, S. *J. Phys. Chem. B* **2006**, *110*, 24011. (e) Finazzi, E.; Di Valentin, C. *J. Phys. Chem. C* **2007**, *111*, 9275. (f) Graciani, J.; Álvarez, L. J.; Rodriguez, J. A.; Sanz, J. F. *J. Phys. Chem. C* **2008**, *112*, 2624.

(33) For example: (a) Irie, H.; Watanabe, Y.; Hashimoto, K. *J. Phys. Chem. B* **2003**, *107*, 5483. (b) Sakthivel, S.; Janczarek, M.; Kisch, H. *J. Phys. Chem. B* **2004**, *108*, 19384. (c) Mrowetz, M.; Balcerski, W.; Colussi, A. J.; Hoffmann, M. R. *J. Phys. Chem. B* **2004**, *108*, 17269. (d) Sakthivel, S.; Kisch, H. *ChemPhysChem.* **2003**, *4*, 487. (e) Kisch, H.; Sakthivel, S.; Janczarek, M.; Mitoraj, D. *J. Phys. Chem. C* **2007**, *111*, 11445. (f) Kuznetsov, V. N.; Serpone, N. *J. Phys. Chem. B* **2006**, *110*, 25203. (g) Serpone, N. *J. Phys. Chem. B* **2006**, *110*, 24287. (h) Livraghi, S.; Paganini, M. C.; Giamello, E.; Selloni, A.; Valentin, C. D.; Pacchioni, G. *J. Am. Chem. Soc.* **2006**, *128*, 15666. (i) Valentin, C. D.; Finazzi, E.; Pacchioni, G.; Selloni, A.; Livraghi, S.; Paganini, M. C.; Giamello, E. *Chem. Phys.* **2007**, *339*, 44. (j) Chen, X. B.; Burda, C. *J. Am. Chem. Soc.* **2008**, *130*, 5018.

(34) (a) Chen, X.; Burda, C. *J. Phys. Chem. B* **2004**, *108*, 15446. (b) Sathish, M.; Viswanathan, B.; Viswanath, R. P.; Gopinath, C. S. *Chem. Mater.* **2005**, *17*, 6349. (c) Chen, H.; Nambu, A.; Wen, W.; Graciani, J.; Zhong, Z.; Hanson, J.; Fujita, E. *J. Phys. Chem. C* **2007**, *111*, 1366. (d) Martínez-Ferrero, E.; Sakatani, Y.; Boissiere, C.; Grosso, D.; Fuertes, A.; Fraxedas, J.; Sanchez, C. *Adv. Funct. Mater.* **2007**, *17*, 3348. (e) Xie, Y.; Li, Y.; Zhao, X. *J. Mol. Catal. A: Chem.* **2007**, *277*, 119. (f) Kisch, H.; Sakthivel, S.; Janczarek, M.; Mitorraj, D. *J. Phys. Chem. C* **2007**, *111*, 11445. (g) Wang, J.; Zhu, W.; Zhang, Y.; Liu, S. *J. Phys. Chem. C* **2007**, *111*, 1010. (h) Chi, B.; Zhao, L.; Jin, T. *J. Phys. Chem. C* **2007**, *111*, 6189. (i) Chen, C.; Bai, H.; Chang, C. *J. Phys. Chem. C* **2007**, *111*, 15228. (j) Cong, Y.; Zhang, J.; Chen, F.; Anpo, M. *J. Phys. Chem. C* **2007**, *111*, 6976.

(35) Kitano, M.; Funatsu, K.; Matsuoka, M.; Ueshima, M.; Anpo, M. *J. Phys. Chem. B* **2006**, *110*, 25266.

modify the electronic structure of the whole titanate particle, thus enhancing photon harvest in the visible-light range. We confirmed our hypotheses both experimentally and by first-principles electronic structure calculations. Homogenous substitution of O by N was achieved in layered cesium titanate via a simple and straightforward nitrogen-doping process, thus resulting in extraordinary band-to-band excitation in the visible-light range up to 472 nm, which has never been attained in any titanate materials. Fundamental insights based on various characterization techniques suggest that the two key features—layered structure and homogeneous doping—are responsible for inducing the extraordinary band-to-band photon excitation and the red-shift to the visible light region.

## 2. Experimental Section

**2.1. Synthesis of the Materials.** The layered titanate compound of $Cs_{0.68}Ti_{1.83}O_4$ was prepared according to a reported procedure.[36] Nitrogen doping in this layered titanate was achieved by simply treating the white $Cs_{0.68}Ti_{1.83}O_4$ powders at 750 °C in ammonia atmosphere, resulting in a light yellow colored sample, herein designated as $Cs_{0.68}Ti_{1.83}O_{4-x}N_x$. Protonated layered compound of $H_{0.68}Ti_{1.83}O_{4-x}N_x$ was prepared by ion-exchange of the $Cs_{0.68}Ti_{1.83}O_{4-x}N_x$ with $H^+$ in 1 mol $L^{-1}$ HCl solution for 3 days.

**2.2. Experimental Methods.** The measurements of the amount of •OH were conducted according to the literature.[37] One-hundred milligrams of photocatalyst was suspended in 80 mL of aqueous solution containing 10 mM NaOH and 3 mM terephthalic acid. Before exposure to visible light irradiation, the suspension was stirred in the dark for 30 min. Then, 5 mL of the solution was taken out every 15 min and centrifuged for fluorescence spectrum measurements. When additional 5 mM $K_2S_2O_8$ was introduced into the above aqueous solution as electron scavenger, the solution was thoroughly degassed with nitrogen gas bubbling to reduce dissolved oxygen molecules prior to the irradiation for 30 min and throughout the photoreaction process. The employed excitation light in recording fluorescence spectra was 320 nm. The photocatalytic performance tests were carried out by adding 100 mg of titanate sample into 100 $cm^3$ of $4 \times 10^{-5}$ mol $L^{-1}$ rhodamine G solution. The suspension was stirred in dark for 30 min to ensure the saturated adsorption of rhodamine G before illumination. The light source was a 300 W Xe lamp (Beijing Trusttech Co., Ltd, PLS-SXE-300UV) with cutoff by a combination of two glass filters with the ranges of 200−770 nm and >420 nm, respectively. For comparison, benchmark titania P25 and nitrogen-doped P25 were also examined using the same testing procedure.

**2.3. Computational Details.** Spin-polarized DFT calculations were carried out to investigate the microscopic and electronic structures of the substitutional doping of N in the crystal of cesium titanate and protonated titanate. The geometry optimization was carried out using the local orbital functional method implemented with the Dmol3 package.[38a] All electron calculations with scalar relativistic corrections were used together with the numerical DNP basis set. Exchange and correlation were treated in the generalized gradient approximation (GGA) of Perdew−Burke−Ernzerhof (PBE).[38b] Optimization of atomic positions were performed on alternate cycles using the BFGS method until the convergence criteria were met (maximum energy change per atom = $1.0 \times 10^{-6}$ eV, maximum rms force = 0.03 eV $Å^{-1}$, maximum rms stress = 0.02 GPa, and maximum rms displacement = $5.0 \times 10^{-4}$ Å). On the basis of the optimized structures, densities of states (DOS) and projected DOS were calculated using the CASTEP package.[38c] The electronic core wave function was described using the standard ultrasoft pseudopotentials available with the package. The k-point set used to sample the reciprocal space was generated using a Monkhurst-Pack grid ($4 \times 4 \times 4$).[38d] PBE functional was used to model electronic exchange and correlation. The SCF tolerance was set as $1.0 \times 10^{-6}$ eV/atom.

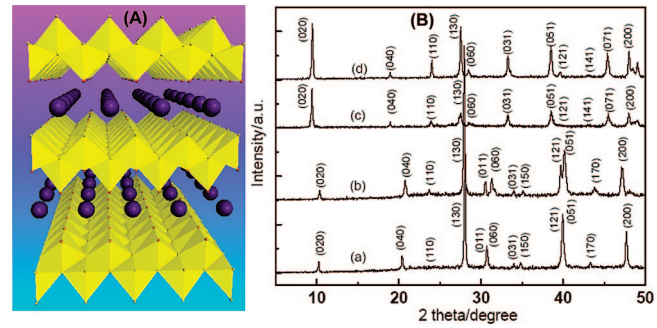


**Figure 1.** (A) Crystal structure model of typical lepidocrocite-type titanate and (B) XRD patterns of (a) $Cs_{0.68}Ti_{1.83}O_4$, (b) $Cs_{0.68}Ti_{1.83}O_{4-x}N_x$, (c) $H_{0.68}Ti_{1.83}O_4$, and (d) $H_{0.68}Ti_{1.83}O_{4-x}N_x$.

## 3. Results and Discussion

**3.1. Crystal Structure of Layered Titanate.** Alkali- and protonated-titanates have a typical lepidocrocite-type layered structure (shown in Figure 1A). Two layers of the network of $TiO_6$ octahedra sharing four edges are nested into a zigzag sheet as the structure unit of the layered titanate, which is also the basic unit of anatase titania. In a typical structure of titanate, the zigzag sheets are separated by alkali ions or hydrated proton as interlayer counterions. The XRD patterns, shown in Figure 1B, confirm the well-retained layered structure of cesium- and protonated-titanate after both nitrogen doping and proton-exchange. The interlayer spacings for $Cs_{0.68}Ti_{1.83}O_{4-x}N_x$ and $H_{0.68}Ti_{1.83}O_{4-x}N_x$ are 8.55 and 9.33 Å, which are consistent with the reported results for undoped $Cs_{0.68}Ti_{1.83}O_4$ and $H_{0.68}Ti_{1.83}O_4$,[36] indicating nitrogen doping has negligible effect on the layered structure of the materials. The resultant nitrogen-doped titanate has an average particle size of ca. 300 nm (Figures S1 and S2 in the Supporting Information).

**3.2. Chemical State and Homogeneity of Substitutional Nitrogen.** To investigate the states of dopant N, we conducted the measurements of N 1s core levels using XPS technique. As shown in Figure 2, no signal for nitrogen species is observed for $Cs_{0.68}Ti_{1.83}O_4$. After nitrogen doping, an additional peak centered at 395 eV appears. Upon ion exchange from $Cs_{0.68}Ti_{1.83}O_{4-x}N_x$ to $H_{0.68}Ti_{1.83}O_{4-x}N_x$, this peak shifts to a higher binding energy of 396.2 eV accompanied by a new peak at 401.5 eV. Although nitrogen doping and related chemical states of nitrogen have been widely investigated in nitrogen-doped $TiO_2$, there are many divergent reports of the states of doped N in titania with variable binding energy ranging from ca. 396 to ca. 402

(36) Sasaki, T.; Watanabe, M.; Hashizume, H.; Yamada, H.; Nakazawa, H. *J. Am. Chem. Soc.* **1996**, *118*, 8329.
(37) Hirakawa, T.; Nosaka, Y. *Langmuir* **2002**, *18*, 3247.
(38) (a) Delley, B. *J. Chem. Phys.* **2000**, *114*, 7756. (b) Perdew, J. P.; Burke, K.; Ernzerhof, M. *Phys. Rev. Lett.* **1996**, *77*, 3865. (c) Payne, M. C.; Teter, M. P.; Allan, D. C.; Arias, T. A.; Joannopoulos, J. D. *Rev. Mod. Phys.* **1992**, *64*, 1045. (d) Monkhorst, H. J.; Pack, J. D. *Phys. Rev. B* **1976**, *13*, 5188.

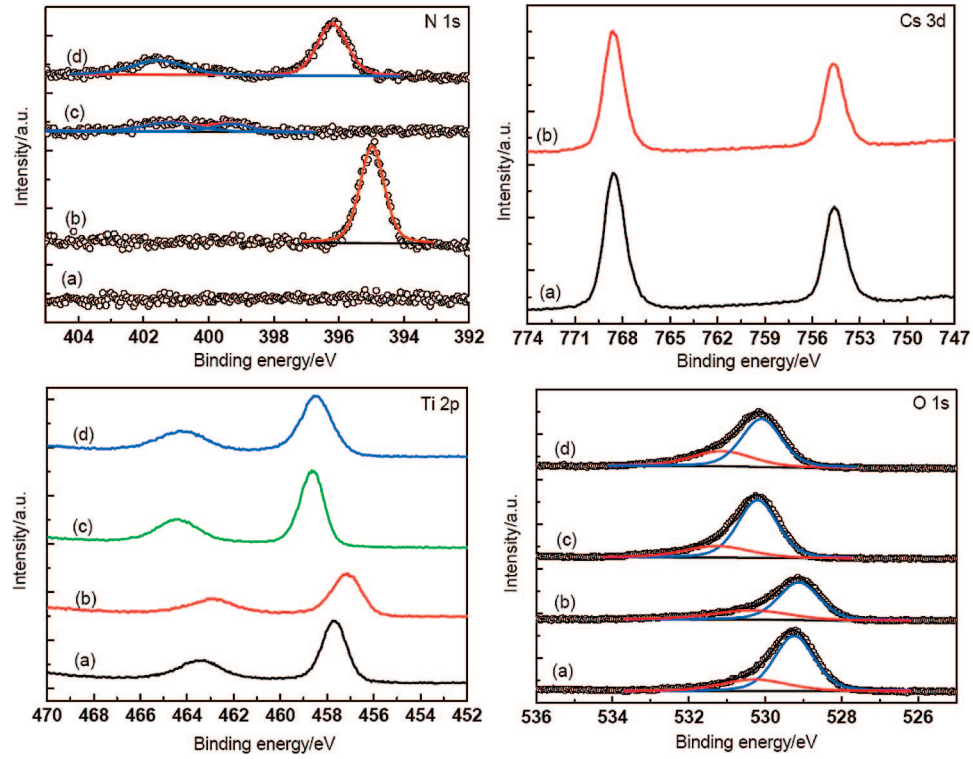


**Figure 2.** High-resolution XPS spectra of N 1s, Cs 3d, Ti 2p, and O 1s measured on the pristine surface of (a) $Cs_{0.68}Ti_{1.83}O_4$ (b), $Cs_{0.68}Ti_{1.83}O_{4-x}N_x$, (c) $H_{0.68}Ti_{1.83}O_4$, and (d) $H_{0.68}Ti_{1.83}O_{4-x}N_x$.

eV.[24a,25−28,34] Generally speaking, doped N with the binding energy at ca. 396 eV is considered to be atomic $\beta$-N,[24a] namely the formation of Ti−N bonds in the network of Ti−O−Ti, but the exact state of nitrogen with its binding energy around 400 eV still needs further investigations even though many reports[34a,b,j] described such nitrogen species as O−Ti−N bonds. In the case of nitrogen-doped Cs and H titanates, similar structure unit consisting of bilayers of $TiO_6$ octahedra to that in anatase $TiO_2$ means that the state of dopant nitrogen should be close to that in anatase $TiO_2$. Therefore, nitrogen dopants with their binding energy of ca. 395 and 396.2 eV in $Cs_{0.68}Ti_{1.83}O_{4-x}N_x$ and $H_{0.68}Ti_{1.83}O_{4-x}N_x$, respectively, can be reasonably assigned to the atomic $\beta$-N. As for the state of nitrogen species at around 400 and 401 eV in $H_{0.68}Ti_{1.83}O_4$ and $H_{0.68}Ti_{1.83}O_{4-x}N_x$, we tend to believe that it is originated from adsorbed or contaminated nitrogen species.[24a] Because of the insignificant contribution to the modification of electronic structure,[24a] the exact assignment of these nitrogen species was not carried out. The smaller binding energy of 395 eV for $Cs_{0.68}Ti_{1.83}O_{4-x}N_x$ can be understood as the effect of small electronegativity of Cs. The smaller electronegativity of Cs than H in the interlayer galleries can result in a higher outer electron density around N in $Cs_{0.68}Ti_{1.83}O_{4-x}N_x$ and thus lower binding energy of N 1s than $H_{0.68}Ti_{1.83}O_{4-x}N_x$.

We also examined the chemical states of Cs, Ti and O in titanates before and after nitrogen doping, as shown in Figure 2. In cesium titanate, there is no detected binding energy shift for Cs 3d after nitrogen doping, but the binding energies of Ti $2p_{3/2}$ and O 1s are shifted from 457.7 and 529.3 eV to 457.1 and 529.1 eV, respectively. This energy shift can be explained as the increased outer electron densities of Ti and O by substituting lattice O atoms with N atoms of a smaller electronegativity (3.44 versus 3.04). Similar shift toward lower binding energy in nitrogen-doped commercial P25 titania and colloidal titania nanoparticles was also reported for Ti and O.[34a] However, the binding energy shift of Ti and O in protonated titanate after nitrogen doping is only 0.1 eV. This much smaller shift is ascribed to the greatly weakened effect of substitutional N on increasing outer electron density of Ti and O by H with stronger electronegativity in the galleries. Another notable characteristic is the obviously broadened Ti 2p peak after nitrogen doping in both $Cs_{0.68}Ti_{1.83}O_{4-x}N_x$ and $H_{0.68}Ti_{1.83}O_{4-x}N_x$ probably due to the formation of Ti−N bond.[27e,f]

The homogeneous distribution of doped N in the whole $H_{0.68}Ti_{1.83}O_{4-x}N_x$ crystals was revealed by time-dependent ion etching of surface layers, as shown in Figure 3(A). The amount of nitrogen dopant was estimated to be ca. 3 at% in $H_{0.68}Ti_{1.83}O_{4-x}N_x$. The unchanged nitrogen amount in $H_{0.68}Ti_{1.83}O_{4-x}N_x$ as that in $Cs_{0.68}Ti_{1.83}O_{4-x}N_x$ (also ca. 3 at%) indicates the stability of nitrogen dopant in layered titanate upon ion exchange. As expected, the obvious reason for the uniform distribution of N dopant in the whole crystal with an average size of 300 nm is the existence of interlayer galleries, which can efficiently facilitate the nitridation process. The space between two neighboring layers allows species such as N/N−H/N−$H_2$ derived from the decomposition of $NH_3$ molecules migrate into the galleries to replace O in $TiO_6$ octrahedra readily and uniformly. It should be mentioned that this process is very different from nitrogen doping in three-dimensional anatase particles, which leads only to a gradient distribution of dopant N on the outer surfaces.

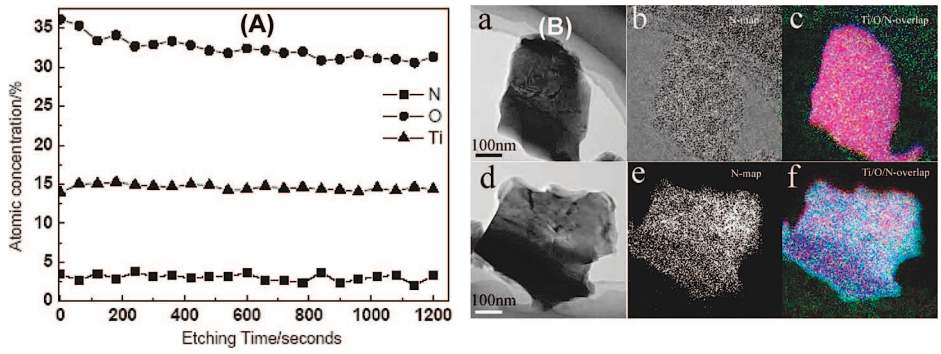


**Figure 3.** (A) XPS depth profiles of the elements of Ti, O and N in the $H_{0.68}Ti_{1.83}O_{4-x}N_x$ upon $Ar^+$ sputtering. (B) Energy-filtered TEM images of (a, d) general morphology, (b, e) N map, and (c, f) Ti/O/N overlapped maps of (a−c) $Cs_{0.68}Ti_{1.83}O_4$ and (d−f) $Cs_{0.68}Ti_{1.83}O_{4-x}N_x$, respectively.

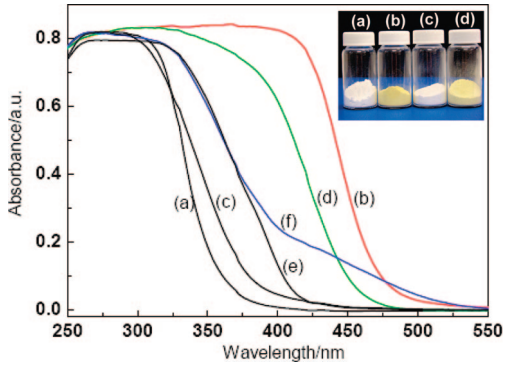


**Figure 4.** UV−visible light absorption spectra of (a) $Cs_{0.68}Ti_{1.83}O_4$, (b) $Cs_{0.68}Ti_{1.83}O_{4-x}N_x$, (c) $H_{0.68}Ti_{1.83}O_4$, (d) $H_{0.68}Ti_{1.83}O_{4-x}N_x$, (e) commercial P25 titania, and (f) nitrogen-doped P25 prepared by calcining P25 powders in ammonia atmosphere at 550 °C for 1 h. The inset is the photos of samples (a) $Cs_{0.68}Ti_{1.83}O_4$, (b) $Cs_{0.68}Ti_{1.83}O_{4-x}N_x$, (c) $H_{0.68}Ti_{1.83}O_4$, and (d) $H_{0.68}Ti_{1.83}O_{4-x}N_x$.

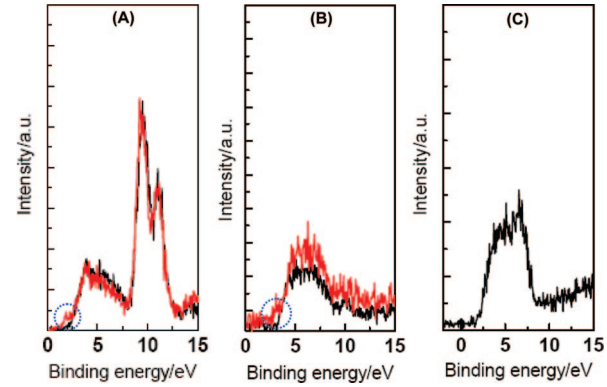


**Figure 5.** Valence band spectra of the photocatalysts. (A) $Cs_{0.68}Ti_{1.83}O_4$ (black) and $Cs_{0.68}Ti_{1.83}O_{4-x}N_x$ (red); (B) $H_{0.68}Ti_{1.83}O_4$ (black) and $H_{0.68}Ti_{1.83}O_{4-x}N_x$ (red); (C) anatase $TiO_2$.

To determine the chemical compositions of the single titanate particle, we used energy-filtered TEM (EFTEM) to show elemental maps of Ti, O, and N in the resultant photocatalysts. Figure 3B presents the typical zero energy loss EFTEM images (Figure 3B-a and 3B-d) of $Cs_{0.68}Ti_{1.83}O_4$ and $Cs_{0.68}Ti_{1.83}O_{4-x}N_x$ particles together with their element mapping images. It is very clear that the N species is uniformly presented in the $Cs_{0.68}Ti_{1.83}O_{4-x}N_x$ particle with very strong contrast (Figure 3B-e), whereas only weak signal intensity is detected in $Cs_{0.68}Ti_{1.83}O_4$ particles (Figure 3B-b). From the overlapped color images of Ti, O, and N maps for $Cs_{0.68}Ti_{1.83}O_{4-x}N_x$ (Figure 3B-f) and $Cs_{0.68}Ti_{1.83}O_4$ (Figure 3B-c), it is further confirmed that N dopant is homogenously distributed in the $Cs_{0.68}Ti_{1.83}O_{4-x}N_x$ particles. Similar results were also obtained for $H_{0.68}Ti_{1.83}O_4$ and $H_{0.68}Ti_{1.83}O_{4-x}N_x$ (not shown).

**3.3. Band-to-Band Photoabsorption and Identification of Electronic Structure.** In contrast to the pristine layered $Cs_{0.68}Ti_{1.83}O_4$ and $H_{0.68}Ti_{1.83}O_4$, the absorbance thresholds of $Cs_{0.68}Ti_{1.83}O_{4-x}N_x$ and $H_{0.68}Ti_{1.83}O_{4-x}N_x$ exhibited an extraordinary band-to-band red shift from 356 and 380 nm to 472 and 453 nm, respectively, very different from the commonly observed small absorbance shoulder in nitrogen-doped titania powders, as shown in Figure 4. The color of $Cs_{0.68}Ti_{1.83}O_4$ and $H_{0.68}Ti_{1.83}O_4$ changed from white to yellow after the nitrogen doping (The inset in Figure 4). The steep absorption edges of $Cs_{0.68}Ti_{1.83}O_{4-x}N_x$ and $H_{0.68}Ti_{1.83}O_{4-x}N_x$ and the almost exactly parallel characteristics of their absorption edges to those of $Cs_{0.68}Ti_{1.83}O_4$ and $H_{0.68}Ti_{1.83}O_4$ strongly suggest the nature of band-to-band excitation in nitrogen-doped $Cs^+$ and $H^+$ titanates, which to the best of our knowledge has never been obtained in titanate materials. The band gaps of $Cs_{0.68}Ti_{1.83}O_4$ and $H_{0.68}Ti_{1.83}O_4$ determined from the plot of the Kubelka−Munk function versus the energy of the light absorbed are 3.62 and 3.47 eV, respectively. After nitrogen doping, the band gap values of $Cs_{0.68}Ti_{1.83}O_{4-x}N_x$ and $H_{0.68}Ti_{1.83}O_{4-x}N_x$ are drastically shifted to 2.73 and 2.85 eV. It is important to note that the nature of band-to-band absorption in nitrogen-doped titanate is independent of the amount of dopant N. However, the absorption threshold of nitrogen-doped titanate is sensitive to the amount of dopant N, and the higher the content of dopant N, the larger the red shift of the threshold.

The relative energy levels of valence band maximum (VBM) and conduction band minimum (CBM) play key roles in determining the redox power of photoinduced carriers in photocatalytic reactions. To determine the effect of nitrogen doping on the positions of CBM and VBM of $Cs_{0.68}Ti_{1.83}O_4$ and $H_{0.68}Ti_{1.83}O_4$, the total densities of states of their valence band were measured (Figure 5). In contrast to undoped titanates, a remarkable change is the upward shift of valence band maximum of $Cs_{0.68}Ti_{1.83}O_{4-x}N_x$ and $H_{0.68}Ti_{1.83}O_{4-x}N_x$ depicted in the blue circles. In particular, the valence band maximums of $Cs_{0.68}Ti_{1.83}O_4$ and $H_{0.68}Ti_{1.83}O_4$ after nitrogen doping are shifted from 2.28 and 3.19 eV to 1.37 and 2.58 eV, respectively. The energy shift of valence band maximum by 0.91 and 0.61 eV in the valence band spectra is well consistent with the band gap shift by 0.89 and 0.62 eV

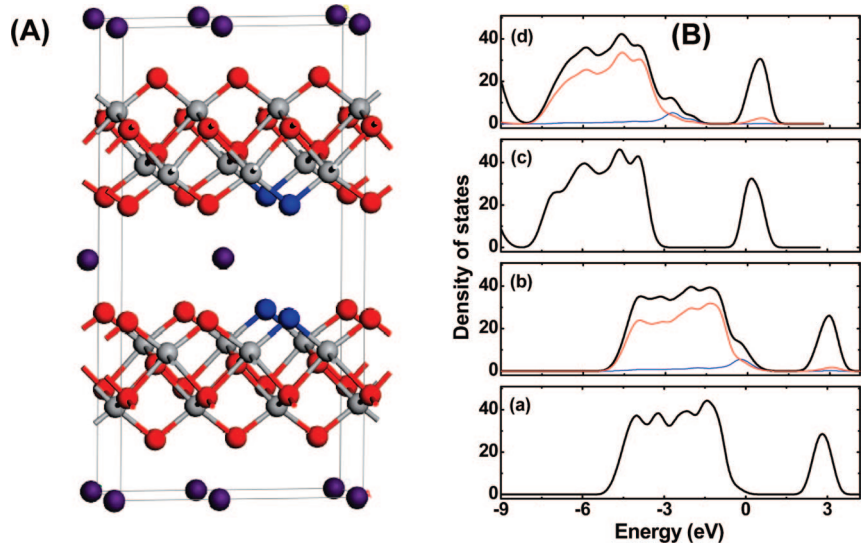


**Figure 6.** (A) Structure model of cesium and protonated titanate. purple color, Cs or H; red, oxygen; gray, titanium; blue, N. (B) Total DOSs (black line) of $Cs_{0.68}Ti_{1.83}O_4$ ( (a)undoped; (b) nitrogen-doped) and $H_{0.68}Ti_{1.83}O_4$ ( (c)undoped; (d) nitrogen-doped) and the projected DOSs of O (red line) and doped N (blue line). The dopant N is located at a substitutional site for four O atoms in the employed models for $Cs_{0.68}Ti_{1.83}O_4$ and $H_{0.68}Ti_{1.83}O_4$ crystals.

determined by UV−visible absorption spectra, for $Cs_{0.68}Ti_{1.83}O_{4-x}N_x$ and $H_{0.68}Ti_{1.83}O_{4-x}N_x$, respectively. The low densities of the newly formed states by nitrogen doping in the valence band are attributed to the low content of substitutional N atoms in relative to O atoms in nitrogen-doped titanates. The valence band maximum of $H_{0.68}Ti_{1.83}O_{4-x}N_x$ is much lower by ca. 1.2 eV than that of $Cs_{0.68}Ti_{1.83}O_{4-x}N_x$, suggesting a much stronger oxidative power of generated holes upon excitation in the former. This characteristic may make $H_{0.68}Ti_{1.83}O_{4-x}N_x$ more efficient in decomposing organic molecules than $Cs_{0.68}Ti_{1.83}O_{4-x}N_x$. Kisch et al.[33d] reported the valence band maximum of anatase $TiO_2$ locating at +2.64 V in reference to normal hydrogen electrode (NHE) at pH 7, and the redox potentials for •OH/$OH^-$ and $O_2/O_2{\bullet}^-$ were determined at +1.9 and −0.33 V.[33c,39] By comparing with the VBM value of 2.01 eV in the valence band of anatase $TiO_2$ (Figure 5C), the electronic potentials for undoped and doped titanates can be determined, as shown in Scheme 1. The oxidative potentials of holes generated in $Cs_{0.68}Ti_{1.83}O_4$ and $H_{0.68}Ti_{1.83}O_4$ are strong enough to oxidize $OH^-$ into •OH. After nitrogen doping, the upward shift of VBM of $Cs_{0.68}Ti_{1.83}O_4$ by around 0.9 eV leads to the potential of holes in $Cs_{0.68}Ti_{1.83}O_{4-x}N_x$ slightly lower than the potential of •OH/$OH^-$. The even lower VBM for $H_{0.68}Ti_{1.83}O_{4-x}N_x$ than anatase by 0.57 eV indicates a stronger oxidative power of holes in photocatalysis oxidation reactions.

**3.4. Calculated Density of States.** To investigate the effect of nitrogen doping on the electronic structure of titanate (as shown in Figure 6A), we calculated densities of states (DOS) and projected DOS of the substitutional N in $H_{0.68}Ti_{1.83}O_4$ and $Cs_{0.68}Ti_{1.83}O_4$ using density functional theory (DFT) and are presented in Figure 6B. On the basis of the calculations, three key insights can be derived. (1) The substitutional doping of N leads to significantly narrowed band gaps instead of some isolated states in the band gap, from 3.22 and 2.55 eV to 1.78 and 1.93 eV for $Cs_{0.68}Ti_{1.83}O_4$ and $H_{0.68}Ti_{1.83}O_4$, respectively. It is well-known that the valance band (VB) and conduction band (CB) of undoped titanate are dominated by $O_{2p}$ and $Ti_{3d}$. With the doping of N, the VB is spanned mainly by $O_{2p}$ and mixed with $N_{2p}$, as shown in Figure 6B-b and B-d, which results in the upshift of VB. Such changes of band gaps are believed to play an important role in both their visible light absorption and photocatalytic activity.[24a] (2) Because of the much lower content of substitutional nitrogen than lattice oxygen in titanate, the contribution of $N_{2p}$ states to the DOS in the new valence band is lower than that of $O_{2p}$ states. (3) Compared to $Cs_{0.68}Ti_{1.83}O_4$ and $Cs_{0.68}Ti_{1.83}O_{4-x}N_x$, $H_{0.68}Ti_{1.83}O_4$, and $H_{0.68}Ti_{1.83}O_{4-x}N_x$ have much deeper VBMs. Importantly, these three points from our calculated results agree well with the revealed information from the UV−visible absorption spectra (Figure 4) and valence band spectra (Figure 5).

**3.5. Visible Light Photocatalytic Activity.** It is vital to demonstrate whether the changed electronic structure induced by homogeneous nitrogen doping would lead to enhanced visible light photocatalytic activity. Most photodecomposition reactions of organic compounds directly utilize the generated holes with sufficient oxidative power in valence band or localized states in the band gap after photoexcitation, or utilize the generated other active species such as important •OH radicals from reaction of holes with surface adsorbed water and hydroxyl group.[17a,b,40,42] It is known that •OH can react with terephthalic acid (TA) to generate 2-hydroxy terephthalic acid (TAOH), which emits unique fluorescence at around 426 nm.[37] As shown in Figure 7, significant fluorescent signals associated with TAOH are generated upon the 420−770 nm visible light irradiation of $Cs_{0.68}Ti_{1.83}O_{4-x}N_x$ and $H_{0.68}Ti_{1.83}O_{4-x}N_x$ suspended in 3 mM TA solution containing 10 mM NaOH for different

(39) Bahnemann, D. W.; Hilgendorff, M.; Memming, R. *J. Phys. Chem. B* **1997**, *101*, 4265.
(40) Bahnemann, D. *Solar Energy* **2004**, *77*, 445.
(41) Anpo, M.; Dohshi, S.; Kitano, M.; Hu, Y.; Takeuchi, M.; Matsuoka, M. *Annu. Rev. Mater. Res.* **2005**, *35*, 1.
(42) Ishibashi, K.; Fujishina, A.; Watanabe, T.; Hashimoto, K. *J. Photochem. Photobiol. A: Chem.* **2000**, *134*, 139.
(43) Li, Q.; Li, Y. W.; Wu, P.; Xie, R.; Shang, J. K. *Adv. Mater.* **2008**, *20*, 3717.

**Scheme 1. Electronic Potential Diagram for Anatase $TiO_2$, $Cs_{0.68}Ti_{1.83}O_4$, $Cs_{0.68}Ti_{1.83}O_{4-x}N_x$, $H_{0.68}Ti_{1.83}O_4$, and $H_{0.68}Ti_{1.83}O_{4-x}N_x$ in Aqueous Solutions at pH 7.0**

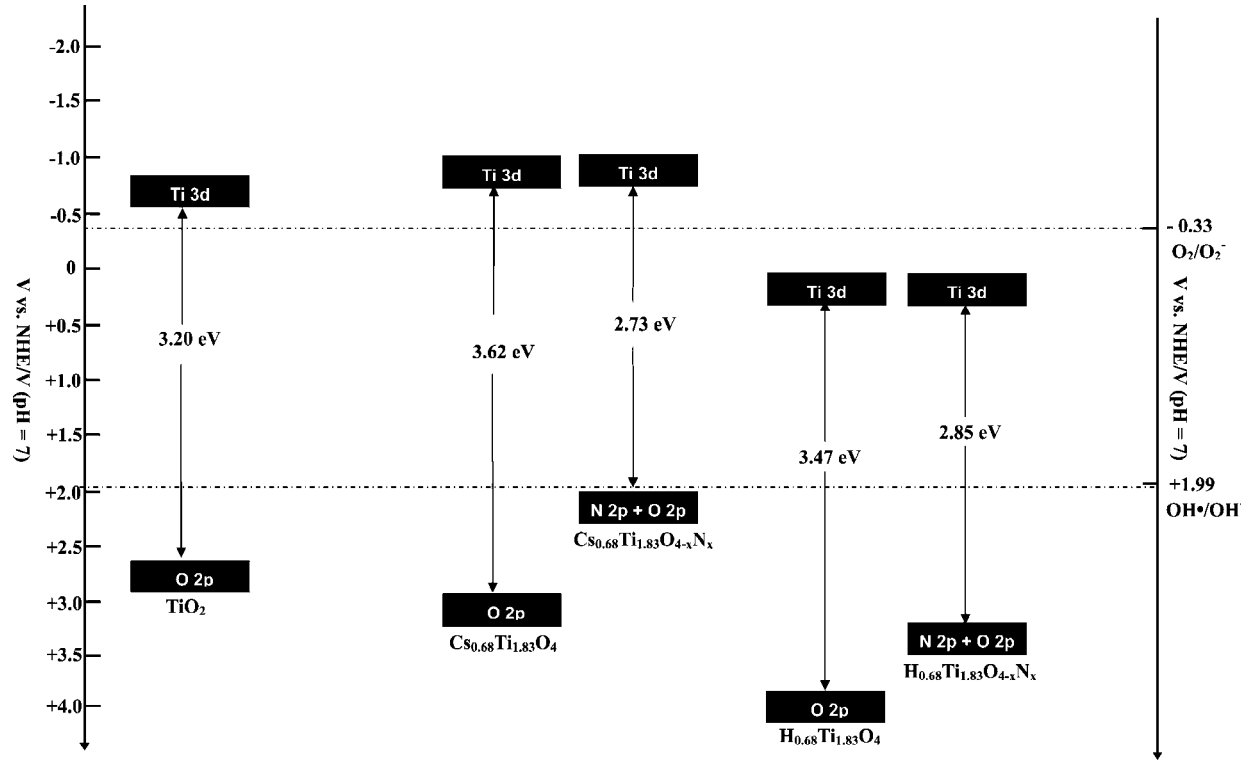


irradiation time. These results clearly show that the generated holes in the newly formed valence bands by nitrogen doping can be easily transferred to surface adsorbed water and hydroxyl groups of doped titanates to generate •OH radicals. The good linear relationship between fluorescence intensity and irradiation time indicates the stability of our homogeneously nitrogen-doped titanates, whereas no signal at all was detected with $Cs_{0.68}Ti_{1.83}O_4$ and $H_{0.68}Ti_{1.83}O_4$ under the same conditions. It should be pointed out that apart from the dominant route of holes attacking water or hydroxyl groups, a secondary route to produce hydroxyl radicals is also possible by the following reactions[43]

$$O_2 + e^- \rightarrow O_2^- \quad (1)$$

$$2O_2^- + 2H^+ \rightarrow 2\bullet OH + O_2 \quad (2)$$

The key in this route is the involvement of protons in the second step. However, the probability of this step should be very low because of the basic medium we used in the experiments. To clarify this point, we investigated the generation of •OH in the aqueous solution containing 5 mM $K_2S_2O_8$ as the electron scavenger, where nitrogen gas flow was bubbled to remove the possible involvement of oxygen molecules prior to and throughout the photocatalytic reactions. The efficient generation of •OH was again observed in this aqueous system because of the trapping of both photoexcited electrons by $S_2O_8^{2-}$ (primary pathway: $S_2O_8^{2-} + e^- \rightarrow SO_4^{-\bullet} + SO_4^{2-}$) and holes by surface adsorbed water molecules and hydroxyl groups. These results strongly confirm that the trapping of holes by surface adsorbed water molecules and hydroxyl groups is the main pathway of active •OH species formation in our case.

An indispensable condition, no matter direct or indirect involvement of holes in photocatalysis reactions, is the efficient consumption of photoexcited electrons by electron acceptors. Single-electron reduction of oxygen ($O_2 + e = O_2^-$(aq), −0.33 V vs NHE; $O_2 + H^+ + e = HO_2$(aq), −0.046 vs NHE) is generally considered as an important pathway to trap photoexcited electrons, where a more negative level of CBM than single-electron reduction potential of oxygen is required.[17a,b] As depicted in Scheme 1, the level of CBM of $Cs_{0.68}Ti_{1.83}O_4$ and $Cs_{0.68}Ti_{1.83}O_{4-x}N_x$ is negative enough to allow single-electron reduction of oxygen, but the level of CBM of $H_{0.68}Ti_{1.83}O_4$ and $H_{0.68}Ti_{1.83}O_{4-x}N_x$ is too positive to proceed this reduction reaction. Thus the nearly linear increase of the amount of •OH in $H_{0.68}Ti_{1.83}O_{4-x}N_x$ upon visible light excitation time (Figure 7B) strongly indicates that the photoexcited electrons in its CB can be efficiently consumed via other reaction paths. It was reported that multielectron reductions of oxygen ($O_2 + 2H^+ + 2e = H_2O_2$(aq), +0.68 vs NHE; $O_2 + 4H^+ + 4e = 2H_2O$(aq), +1.23 V vs NHE) exist in $Pt/WO_3$ system with a more positive level of CBM (+0.5 V vs NHE for $WO_3$) than single-electron reductions of oxygen.[23a] In our system, it is reasonable to deduce that multielectron reductions of oxygen might have occurred because of the electrons in the more negative level of CBM in $H_{0.68}Ti_{1.83}O_{4-x}N_x$ (+0.36 V vs NHE) than the redox potentials of multielectron reductions of oxygen.

The photocatalytic activity of $Cs_{0.68}Ti_{1.83}O_{4-x}N_x$ and $H_{0.68}Ti_{1.83}O_{4-x}N_x$ was further evaluated by photodegradation of a model organic pollutant rhodamine G under the irradiation of visible light between the wavelength of 420 and 770 nm. Interestingly, $Cs_{0.68}Ti_{1.83}O_{4-x}N_x$ with an average

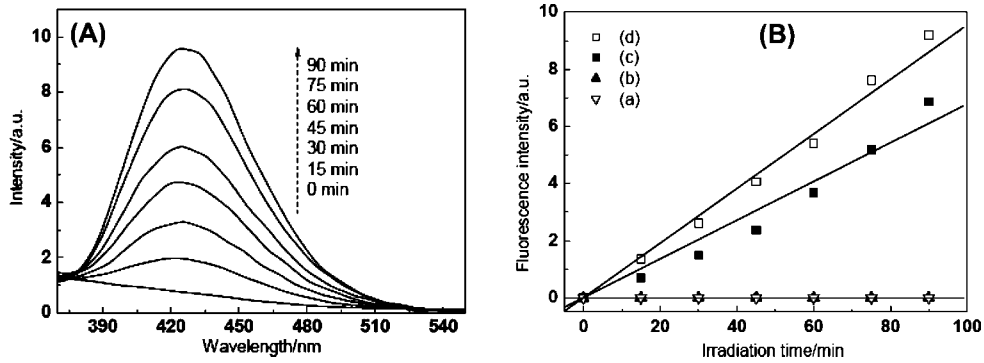


**Figure 7.** (A) Fluorescence spectra of the visible-light (420−770 nm) irradiated $H_{0.68}Ti_{1.83}O_{4-x}N_x$ suspension in 3 mM terephthalic acid at different irradiation time; (B) time dependences of the fluorescence intensity at 426 nm with different photocatalysts: (a) $Cs_{0.68}Ti_{1.83}O_4$, (b) $H_{0.68}Ti_{1.83}O_4$, (c) $Cs_{0.68}Ti_{1.83}O_{4-x}N_x$ and (d) $H_{0.68}Ti_{1.83}O_{4-x}N_x$.

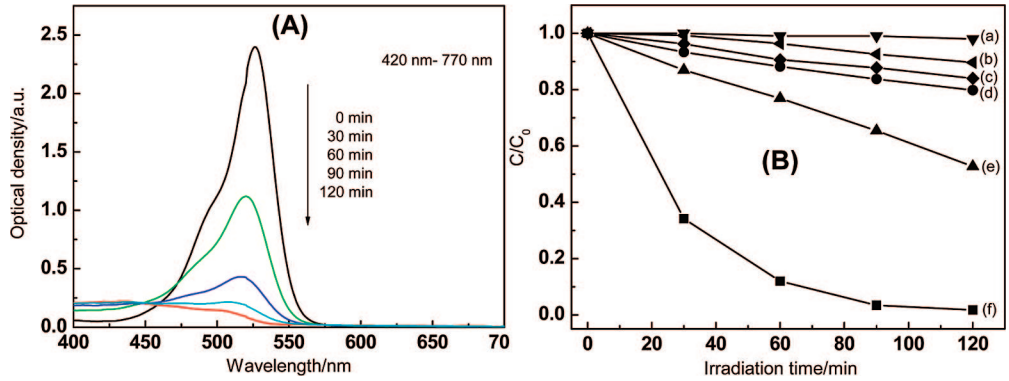


**Figure 8.** Comparison of photocatalytic activity for different photocatalysts. (A) Time evolvement of the absorbance spectrum of Rhodamine G degraded by $H_{0.68}Ti_{1.83}O_{4-x}N_x$ under the irradiation of the wavelength from 420 to 770 nm. (B) Photocatalytic activity of (a) no photocatalyst under visible light irradiation; (b) $Cs_{0.68}Ti_{1.83}O_{4-x}N_x$ and (c) $H_{0.68}Ti_{1.83}O_{4-x}N_x$, in the dark; (d) nitrogen-doped P25, (e) $Cs_{0.68}Ti_{1.83}O_{4-x}N_x$, and (f) $H_{0.68}Ti_{1.83}O_{4-x}N_x$, under visible light.

crystal size of 300 nm and specific surface area of no larger than 2 $m^2\ g^{-1}$ show better photocatalytic activity than both undoped and nitrogen-doped P25 $TiO_2$, and the $H_{0.68}Ti_{1.83}O_{4-x}N_x$ photocatalyst exhibits a much faster photodecomposition rate of rhodamine G under the same conditions, as shown in Figure 8. The highly enhanced visible-light photocatalytic activities of $Cs_{0.68}Ti_{1.83}O_{4-x}N_x$ and $H_{0.68}Ti_{1.83}O_{4-x}N_x$ with such a large crystal size and small surface areas are clearly attributed to their unique layered structures and the homogeneous distribution of dopant N in the layered titanates, which significantly contributes to the band-to-band visible-light excitation, and hence substantially enhances the visible-light absorption and higher mobility of photoexcited carriers.

Compared to $Cs_{0.68}Ti_{1.83}O_{4-x}N_x$, protonated $H_{0.68}Ti_{1.83}O_{4-x}N_x$ has three potential advantages: (1) its considerably larger specific surface area (12 $m^2g^{-1}$ versus 2 $m^2\ g^{-1}$); (2) the higher ratio of active $TiO_6$ octahedra sheets in a unit mass (99.55% versus 62.69%); (3) the stronger oxidative power (3.21 versus 2.00 V at pH 7) of the generated holes in the newly formed valence band upon visible light irradiation. Because the amount of generated •OH from $H_{0.68}Ti_{1.83}O_{4-x}N_x$ is only slightly higher than that from $Cs_{0.68}Ti_{1.83}O_{4-x}N_x$ (Figure 7), which is therefore not the only reason for higher activity of $H_{0.68}Ti_{1.83}O_{4-x}N_x$. Another photocatalytic reaction pathway, i.e., the direct involvement of holes with much stronger oxidative power in attacking and decomposing substrate molecules, can be attributable to the faster degradation process of organic molecules for $H_{0.68}Ti_{1.83}O_{4-x}N_x$.[17a,b,40−42]

In addition, we found that the homogeneous nitrogen-doped layered titanate photocatalysts have high photocatalytic stability. Recycling tests for 4 times show only around 5% activity reduction. After reactions, both the crystal structure of the titanates and the content and chemical state of nitrogen dopant can be well retained. The simple process of nitrogen doping and ion exchange is also a merit worth noting from the viewpoints of photocatalyst scale-up production and low cost for practical applications.

## 4. Conclusions

Homogeneous nitrogen doping was realized in layered titanates for the first time, which leads to extraordinary band-to-band visible light excitation and high visible light photocatalytic activity. This efficient doping strategy distinctly decreases the bandgaps of $Cs_{0.68}Ti_{1.83}O_4$/$H_{0.68}Ti_{1.83}O_4$ from 3.62/3.47 to 2.73/2.85 eV. A small proportion of mixed N 2p states with O 2p states as evidenced by photoelectron spectroscopy and first-principles calculations is confirmed to be responsible for the upshift of valence band maximum of $Cs_{0.68}Ti_{1.83}O_{4-x}N_x$ and $H_{0.68}Ti_{1.83}O_{4-x}N_x$. The much stronger oxidative potential of generated holes in $H_{0.68}Ti_{1.83}O_{4-x}N_x$ upon visible light excitation by around 1.2 V than •OH/$OH^-$ contributes to its high visible-light photocatalytic activity in decom-

posing organic molecules. This finding is of significant importance not only because a highly active visible-light photocatalyst is developed using a simple doping route but it advances the fundamental understanding of the substantial role of uniform nitrogen doping in titania-based photocatalysts. The method is also applicable to the development of uniform anion doping in a number of other layered semiconductors or oxides for applications in sensors, electronic, and optoelectronic devices.

**Acknowledgment.** The financial support from Australian Research Council (through its Centre's grant and DP programs) and Major Basic Research Program, Ministry of Science and Technology of China (2009CB220001) is gratefully acknowledged.

**Supporting Information Available:** SEM images and particle size distributions of photocatalysts $Cs_{0.68}Ti_{1.83}O_{4-x}N_x$ and $H_{0.68}Ti_{1.83}O_{4-x}N_x$ (PDF). This material is available free of charge via the Internet at http://pubs.acs.org.

CM802986R